PDK1 in apical signaling endosomes participates in the rescue of the polarity complex atypical PKC by intermediate filaments in intestinal epithelia

Anastasia Mashukova[a,b], Radia Forteza[a], Flavia A. Wald[a], and Pedro J. Salas[a]
[a]Department of Cell Biology, Miller School of Medicine, University of Miami, Miami, FL 33136; [b]Department of Physiology, College of Medical Sciences, Nova Southeastern University, Fort Lauderdale-Davie, FL 33328

ABSTRACT Phosphorylation of the activation domain of protein kinase C (PKC) isoforms is essential to start a conformational change that results in an active catalytic domain. This activation is necessary not only for newly synthesized molecules, but also for kinase molecules that become dephosphorylated and need to be refolded and rephosphorylated. This "rescue" mechanism is responsible for the maintenance of the steady-state levels of atypical PKC (aPKC [PKCι/λ and ζ]) and is blocked in inflammation. Although there is consensus that phosphoinositide-dependent protein kinase 1 (PDK1) is the activating kinase for newly synthesized molecules, it is unclear what kinase performs that function during the rescue and where the rescue takes place. To identify the activating kinase during the rescue mechanism, we inhibited protein synthesis and analyzed the stability of the remaining aPKC pool. PDK1 knockdown and two different PDK1 inhibitors—BX-912 and a specific pseudosubstrate peptide—destabilized PKCι. PDK1 coimmunoprecipitated with PKCι in cells without protein synthesis, confirming that the interaction is direct. In addition, we showed that PDK1 aids the rescue of aPKC in in vitro rephosphorylation assays using immunodepletion and rescue with recombinant protein. Surprisingly, we found that in Caco-2 epithelial cells and intestinal crypt enterocytes PDK1 distributes to an apical membrane compartment comprising plasma membrane and apical endosomes, which, in turn, are in close contact with intermediate filaments. PDK1 comigrated with the Rab11 compartment and, to some extent, with the transferrin compartment in sucrose gradients. PDK1, pT555-aPKC, and pAkt were dependent on dynamin activity. These results highlight a novel signaling function of apical endosomes in polarized cells.

Monitoring Editor
Robert D. Goldman
Northwestern University

Received: Dec 2, 2011
Revised: Feb 14, 2012
Accepted: Feb 29, 2012

INTRODUCTION

Atypical protein kinase C (aPKC, comprising PKCι/λ and PKCζ) is essential for polarization in epithelia and neurons and is conserved in the evolution of multicellular organisms (Suzuki and Ohno, 2006). It is a central component of the Par3-Par6-aPKC polarity complex (Wang and Margolis, 2007). In epithelial cells, it controls the assembly and localization of tight junctions (Suzuki *et al.*, 2002; Tanentzapf and Tepass, 2002). Furthermore, overexpression of aPKC is causative of cancers (Zhang *et al.*, 2006; Fields and Regala, 2007). In addition, we recently demonstrated that proinflammatory signaling downregulates aPKC in intestinal epithelial cells in culture and in vivo and that decreased aPKC activity is sufficient to mimic some of the consequences of tumor necrosis factor-α stimulation (Mashukova *et al.*, 2011). The same mechanism seems to operate in human patients with inflammatory bowel disease (Wald *et al.*, 2011). Therefore posttranslational mechanisms that regulate steady-state levels of PKCι/λ and PKCζ are of biological and perhaps clinical significance.

Phosphoinositide-dependent kinase 1 (PDK1) activates several kinases, including newly synthesized PKC isoforms, by phosphorylation of the activation domain. It is a well-established component of

This article was published online ahead of print in MBoC in Press (http://www.molbiolcell.org/cgi/doi/10.1091/mbc.E11-12-0988) on March 7, 2012.

Address correspondence to: Pedro J. Salas (psalas@miami.edu).

Abbreviations used: aPKC, atypical protein kinase C (PKCι/λ and ζ); IF, intermediate filament; Krt, keratin; PDK1, phosphoinositide-dependent protein kinase 1; PI3K, phosphatidylinositol 3-kinase; PKC, protein kinase C; Tfn, transferrin.

the phosphatidylinositol 3-kinase (PI3K)–Akt pathway (Pearce *et al.*, 2010). In the case of aPKC isoforms, it was shown that PDK1 exerts a priming phosphorylation (Gould and Newton, 2008) in the activation domain (T410) in PKCζ (Balendran *et al.*, 2000), which is followed by autophosphorylation in the turn domain (T555; Newton, 2010). Because the priming phosphorylation in the activation domain is unstable, the ensuing autophosphorylation in T555 is a better reporter for the process (Gould and Newton, 2008). In addition, the turn domain is identical in PKCι and PKCζ, and thus anti-pT555 antibodies recognize both isoforms, that is, all aPKC in the active conformation. PDK1-mediated aPKC phosphorylation, unlike Akt phosphorylation/activation, is phosphoinositide independent (Sonnenburg *et al.*, 2001; Bayascas, 2008). Of importance, PKC isoforms are sensitive to dephosphorylation of the turn domain as a consequence of their own activity. This is further highlighted by the fact that occupation of the nucleotide-binding pocket by inhibitors renders them more stable (Cameron *et al.*, 2009). Moreover, the isoforms that can be overstimulated by phorbol esters (conventional and novel) become more unstable upon stimulation (Leontieva and Black, 2004). Once PKC is dephosphorylated, it becomes Triton X-100 insoluble and binds to Hsc/Hsp70 chaperones. Then PKC either can be ubiquitinylated and degraded or may be "rescued" through Hsp70–mediated refolding and subsequent rephosphorylation (Gao and Newton, 2006).

We recently showed that the same principle of enhanced dephosphorylation by activity applies to PKCι, which became the basis for the biochemical rescue assay (Mashukova *et al.*, 2009). In addition, we demonstrated that the rescue mechanism responsible for maintaining the steady-state levels of aPKC depends on the presence of native filamentous keratin (Krt) intermediate filaments in epithelial cells. Knockdown of either Hsc/Hsp70 or keratins in those cells results in >90% downregulation of aPKC without any changes in transcription. Krt8-knockout mice lacking intermediate filaments (IFs) in intestinal villi showed loss of aPKC in the villi but not in the crypts. Conversely, $Krt18^{+/-}$, $Krt19^{-/-}$, and hKrt18 R89C knockout/knock-in mice lacking IFs in the crypts but not in the villi showed loss of aPKC in the crypts with normal expression in the villi. Finally, transgenic Krt8 overexpressors showing an excess of abnormally localized IFs also showed delocalization of the aPKC signal (Mashukova *et al.*, 2009), normally restricted to the apical region in the wild-type animals (Wald *et al.*, 2008).

Although substantial progress showing the components of the aPKC refolding machinery has been achieved, the kinase involved in the rephosphorylation of the activation domain after chaperone-mediated refolding remains unknown, and its identification was one of the goals of this work. The original data supporting a role of PDK1 in activation domain phosphorylation (Balendran *et al.*, 2000) were obtained before the importance of the rescue mechanism was established and did not distinguish between the phosphorylation of newly synthesized PKC and the rephosphorylation mechanism that follows Hsp70-mediated rescue. Because of the long-half life of aPKC (approximately 24 h; Mashukova *et al.*, 2011), our hypothesis was that these data reflected the involvement of PDK1 not only in phosphorylation of newly synthesized aPKC, but also in rephosphorylation of aPKC as a part of the Hsp70-mediated refolding and rescue mechanism. This hypothesis, however, had a conceptual caveat: active PDK1 is associated to the plasma membrane by phosphatidylinositol (3,4,5)-trisphosphate (PIP3)–dependent and –independent mechanisms (Bayascas, 2008), whereas the rescue mechanism occurs in or around intermediate filaments (Mashukova *et al.*, 2009). In addition, PIP3 is known to be concentrated in the basolateral membrane (Gassama-Diagne *et al.*, 2006), as well as in μ1B/AP-1B–positive, transferrin receptor–positive recycling endosomes (common recycling endosomes [CREs]; Fields *et al.*, 2010). Conversely, it is conceivable that a cytosolic kinase, either PDK1 or a different enzyme, could be responsible for aPKC rephosphorylation and rescue. Thus, to fully understand the aPKC rescue mechanism, it was essential to determine the subcellular localization of the kinase as well.

RESULTS

PDK1 stabilizes atypical PKC steady-state levels under inhibition of protein synthesis

We used Caco-2 cells, a human colon carcinoma cell line that polarizes and differentiates well in culture. PKCι is very stable in Caco-2 cells, with half-life of >24 h estimated by metabolic labeling studies (Mashukova *et al.*, 2011). To determine the identity of the kinase involved in aPKC rescue, we took advantage of the long half-life of phosphorylated (active conformation) PKC (Smith *et al.*, 2003; Pearce *et al.*, 2010), as opposed to the unstable, nonphosphorylated forms (Balendran *et al.*, 2000). We applied that information to analyze the pool of aPKC, which persists for hours during inhibition of protein synthesis. PKCζ, the other aPKC isoform, also persists for >24 h in the presence of cycloheximide (Le Good and Brindley, 2004). To test the hypothesis that PDK1 is involved in rescue in addition to its role in activating newly synthesized protein, we used two PDK1 inhibitors. After 24 h in cycloheximide, there was an ~50% decrease in PKCι (Figure 1, A–C), consistent with the turnover of the protein. Treatment with nonphosphorylatable PDK1 pseudosubstrate myristoylated peptide (Gao and Harris, 2006; nonphosphorylatable by changing the target Thr for an Ala, iPDK1-tide) greatly reduced the level of PKCι below its turnover (cycloheximide alone) levels (Figure 1A). In addition, incubation with the commonly used PDK1 inhibitor BX-912 (Peifer and Alessi, 2008), alone or in the presence of cycloheximide, reduced the levels of PKCι by 86% as compared with control and 70% below the levels of the treatment with cycloheximide alone (Figure 1, B and C). Phosphorylation of Akt induced by epidermal growth factor (EGF) was used as a positive control for the effect of these pharmacological inhibitors. Conversely, the mTORC2 inhibitor rapamycin failed to destabilize PKCι (Figure 1, A–C), although this drug affects the phosphorylation of the turn domain in conventional and novel PKC isoforms (Ikenoue *et al.*, 2008).

To ensure that the destabilization of PKCι was PDK1 specific, we knocked down this protein with short hairpin RNA (shRNA) delivered by lentivirus particles. The efficiency of the knockdown estimated by immunoblot was approximately 87% (Figure 1D). Of importance, although the PDK1-knockdown cells grew at a much slower rate than the mock-infected controls, we could not detect apoptosis by caspase 3 cleavage (Figure 1D). We performed a 24-h time course after addition of cycloheximide. Once again, mock-transduced cells showed a PKCι degradation rate over a 24-h period (Figure 1, D and E) consistent with the normal turnover of the protein (Mashukova *et al.*, 2011). As expected, the PKCι levels in the knockdown cells were significantly lower than in the control cells (Figure 1E, 0 h). In the presence of cycloheximide, however, the levels of PKCι became indistinguishable from the background at 8 h, with an at least sixfold reduction in the apparent half-life of the protein (Figure 1E).

PDK1 interacts directly with PKCι

Although it is broadly accepted that the activation domain of several PKC isoforms is a direct target of PDK1, we sought to verify this specifically for PKCι in our cells, since no published data were available. It was especially important to test whether the direct interaction remains under inhibition of protein synthesis, because it is conceivable that upstream controls of PDK1 may be affected by

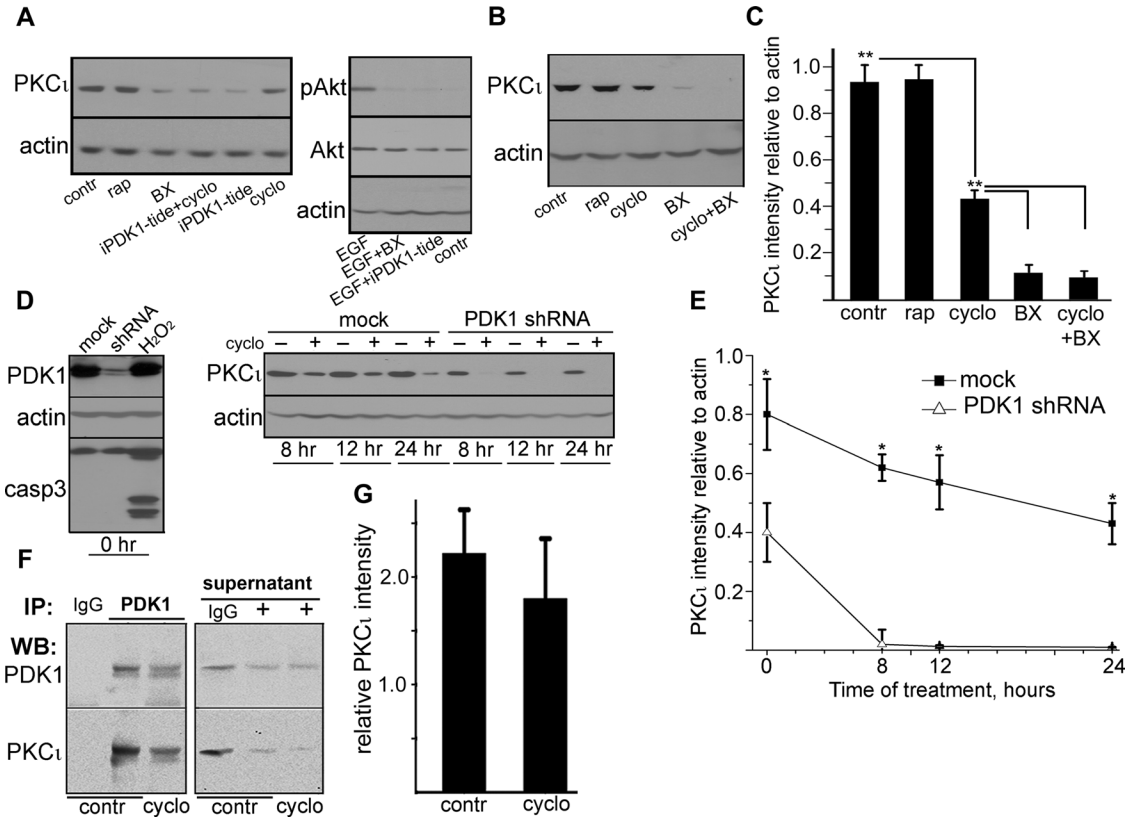

FIGURE 1: PDK1 coimmunoprecipitates with and sustains steady-state levels of PKCι under protein synthesis inhibition. (A) Confluent, differentiated Caco-2 cells were treated with 10 μg/ml cycloheximide (cyclo), 100 nM rapamycin (rap; mTOR inhibitor), 0.5 μM BX-912 (BX; PDK1 inhibitor), 50 μM myristoylated PDK1 inhibitory pseudosubstrate peptide (iPDK1-tide), or none (contr) for 24 h. EGF-induced phosphorylation of Akt in parallel cultures was used as a positive control for the effect of both PDK1 inhibitors in the absence of cycloheximide. (B) In a similar experiment BX-912 was used in the presence of cycloheximide (last lane), or all three drugs were used separately. (C) The values from bands in three independent experiments as described in B were expressed as a ratio to the corresponding actin band (loading control) in the same lanes. Statistical significance was determined by Student's *t* tests of pairs of means; *$p < 0.025$ and **$p < 0.005$ indicate the probability of random differences from the average value immediately above ($n = 3$). (D) Caco-2 cells were transduced with mock lentiviral particles (mock) or with particles expressing anti-PDK1 shRNA and selected in puromycin. Confluent, differentiated cells not exposed to cycloheximide (0 h) were used to assess the efficacy of the knockdown and to control for apoptosis with anti–caspase 3 (casp3) antibody. A 2-h incubation in 20 mM H_2O_2 of mock cells served as a positive control for apoptosis. Cells were treated (+) or not (–) with 10 μg/ml cycloheximide for indicated periods of time for up to 24 h. Total SDS extracts were analyzed by immunoblotting with the antibodies indicated on the left. (E) The values from bands in three independent experiments as described in D were expressed as described in C and plotted as a function of time. (F) For coimmunoprecipitation experiments, Caco-2 cells were incubated or not (contr) with 10 μg/ml cycloheximide overnight (cyclo). The Triton-soluble fraction was immunoprecipitated with rabbit polyclonal anti-PDK1 antibody (+) or with nonimmune IgG, and analyzed by immunoblot for PDK1 or PKCι. The same blot analysis was performed for samples of the supernatant after the immunoprecipitation. (G) Relative amount of PKCι immunoprecipitated with PDK1 was calculated by normalizing the PKCι signal to the PDK1 signal in the same immunoprecipitates. Data represent the mean ± SD from three independent experiments. The averages of PKCι immunoprecipitated in the presence or absence of cycloheximide were not significantly different.

prolonged treatment in cycloheximide. To this end, we immunoprecipitated PDK1 in control cells, as well as in cells that had been incubated in cycloheximide (cyclo) for 24 h from the Triton X-100–soluble fraction. In both cases, PKCι coimmunoprecipitated with PDK1 (Figure 1, F and G) without significant differences between the groups.

PDK1 is necessary and sufficient to rescue dephosphorylated aPKC on intermediate filaments

Because the Hsp70 chaperoning activity necessary for aPKC refolding during the rescue process is associated with the intermediate filament cytoskeleton (Mashukova *et al.*, 2009), we used a fractionation procedure that separates the entire cell contents into three fractions: S1, Triton X 100 soluble, contains cytosol and membrane components; S2, Triton insoluble and 1.5 M KCl soluble; and P (pellet), which comprises the intermediate filament (IF) cytoskeleton and proteins tightly associated to IFs. Conversely, S1 and S2 contain all the actin and tubulin cytoskeleton, as well as lipid rafts (Mashukova *et al.*, 2009). In all the experiments, equal amounts of protein from all three fractions were used and loaded in the gels (Figure 2A, Ponceau S). It is important to note that with this fractionation procedure no component of the cell is discarded, that is, every protein expressed in the cell is present in one or more of the fractions. aPKC, for example, is present in all three

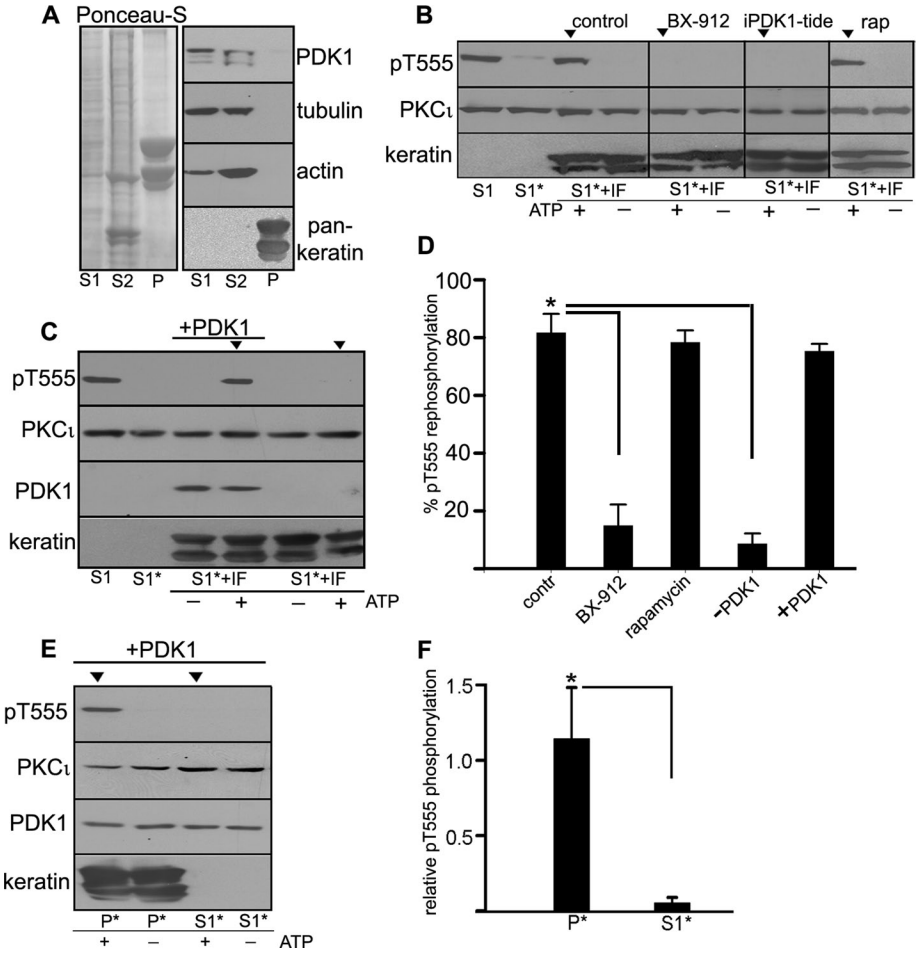

FIGURE 2: PDK1 is necessary for PKCι rephosphorylation in an in vitro reconstitution assay. (A) Confluent, differentiated Caco-2 cells were fractionated in S1 (Triton X-100 soluble), S2 (Triton X-100 insoluble, 1.5 M KCl soluble) and P (post–1.5 M KCl pellet) fractions. In all gels identical amounts of protein from each fraction were used per lane. Protein load is shown by Ponceau S staining of the entire blot, and relative distribution of PDK1, tubulin, actin, and keratins in each fraction are shown by immunoblot. (B) In vitro reconstitution assay. The S1 fraction originally containing pT555 aPKC, was incubated with ATP and aPKC substrate peptide for 4 h, resulting in dephosphorylation of aPKC (S1*) by endogenous phosphatases. Then, the peptide was removed, and the S1* fraction (dephosphorylated aPKC) was supplemented with purified keratin intermediate filaments (S1* + IF) and incubated in the presence of fresh ATP for an additional 4 h. Under control conditions, this results in aPKC rephosphorylation (control, arrowhead). Similar reactions were performed in the presence of 0.5 μM BX-912, 50 μM iPDK1-tide peptide, or 100 nM rapamycin. (C) A similar reconstitution assay was performed using S1 previously immunodepleted in endogenous PDK1. One of the reactions was supplemented with 0.1 μg/ml active recombinant purified PDK1 (+), and it was the only one that sustained aPKC rephosphorylation (arrowhead). (D) Experiments like those in B and C were quantified as intensity of the rephosphorylated T555 relative to the original intensity after extraction (S1). The data are shown as average ± SD (n = 3). Asterisk indicates significance of the difference with regard to the control values, $p < 0.005$. (E) The Caco-2 IF pellet fraction P (which, unlike the purified IF, contains all the IF-associated proteins, including PKCι) was subjected to aPKC dephosphorylation as described (P*) and supplemented with recombinant PDK1. As a control, S1* was supplemented with the same amount of recombinant PDK1. aPKC rephosphorylation was assayed as described. (F) Averages ± SD of pT555/PKCι bands from three independent experiments like the one shown in E. *$p < 0.005$.

fractions (Mashukova *et al.*, 2009). PDK1 distributed in the S1 and S2 fractions, whereas keratins (epithelial IFs) were present only in the P fraction (Figure 2A). Because pT555 aPKC is present in all three fractions (Mashukova *et al.*, 2009), to carry out a rephosphorylation reaction, we dephosphorylate all the fractions first. Dephosphorylation was performed as described (Mashukova *et al.*, 2009) by forcing aPKC kinase activity with ATP and a specific substrate peptide for 4 h in the presence of proteasome and protease inhibitors, but without phosphatase inhibitors. This procedure exposes phospho sites in PKC to endogenous phosphatases. Cell fractions in which aPKC has been dephosphorylated will be noted with an asterisk (e.g., S1*, P*). To proceed with the rephosphorylation, the peptide was removed by ultrafiltration, and ATP was replenished. We previously showed that none of the three fractions alone is capable of rephosphorylating aPKC, but the combination of S1* + P* does sustain aPKC activation domain rephosphorylation in an Hsp70/Hsc70-dependent manner, which can be reported by the ensuing autophosphorylation in T555 (Mashukova *et al.*, 2009). The same type of experiment was repeated here using highly purified IFs in their native, filamentous configuration instead of the P* fraction. Under those conditions, S1* + IF sustained aPKC T555 rephosphorylation only in the presence of ATP (Figure 2B, control arrowhead). Similarly, the mix also resulted in T555 rephosphorylation in the presence of rapamycin, further ruling out a possible involvement of mTORC2. However, the mix failed to rephosphorylate T555 in the presence of the PDK1 inhibitor BX-912 or iPDK1-tide peptide (Figure 2B, BX-912, iPDK1-tide arrowheads).

To independently test the role of PDK1 in aPKC rephosphorylation, we immunodepleted PDK1 in S1 using the same immunoprecipitation protocol shown in Figure 1F but increasing the concentration of immunoprecipitating antibody by threefold. After immunoprecipitation, endogenous PDK1 was undetectable by immunoblot (Figure 2C, S1). This preparation was then dephosphorylated as described previously (Figure 2C, S1*), supplemented with purified IFs, and used in a rephosphorylation assay. aPKC rephosphorylation failed in the absence of PDK1 (Figure 2C, last lane, arrowhead). Conversely, we were able to restore aPKC rephosphorylation by addition of the recombinant purified PDK1 (Figure 2C, +PDK1). The quantification of these results indicated that BX-912 inhibits aPKC rephosphorylation to the same extent as PDK1 immunodepletion in S1 (89%; Figure 3D). It is also important to note that the T555 rephosphorylation assay achieves an average 81% rephosphorylation as compared with the pT555 signal at the beginning of the procedure immediately after cell extraction. In other words, most of the originally phosphorylated aPKC can be resphosphorylated after these procedures.

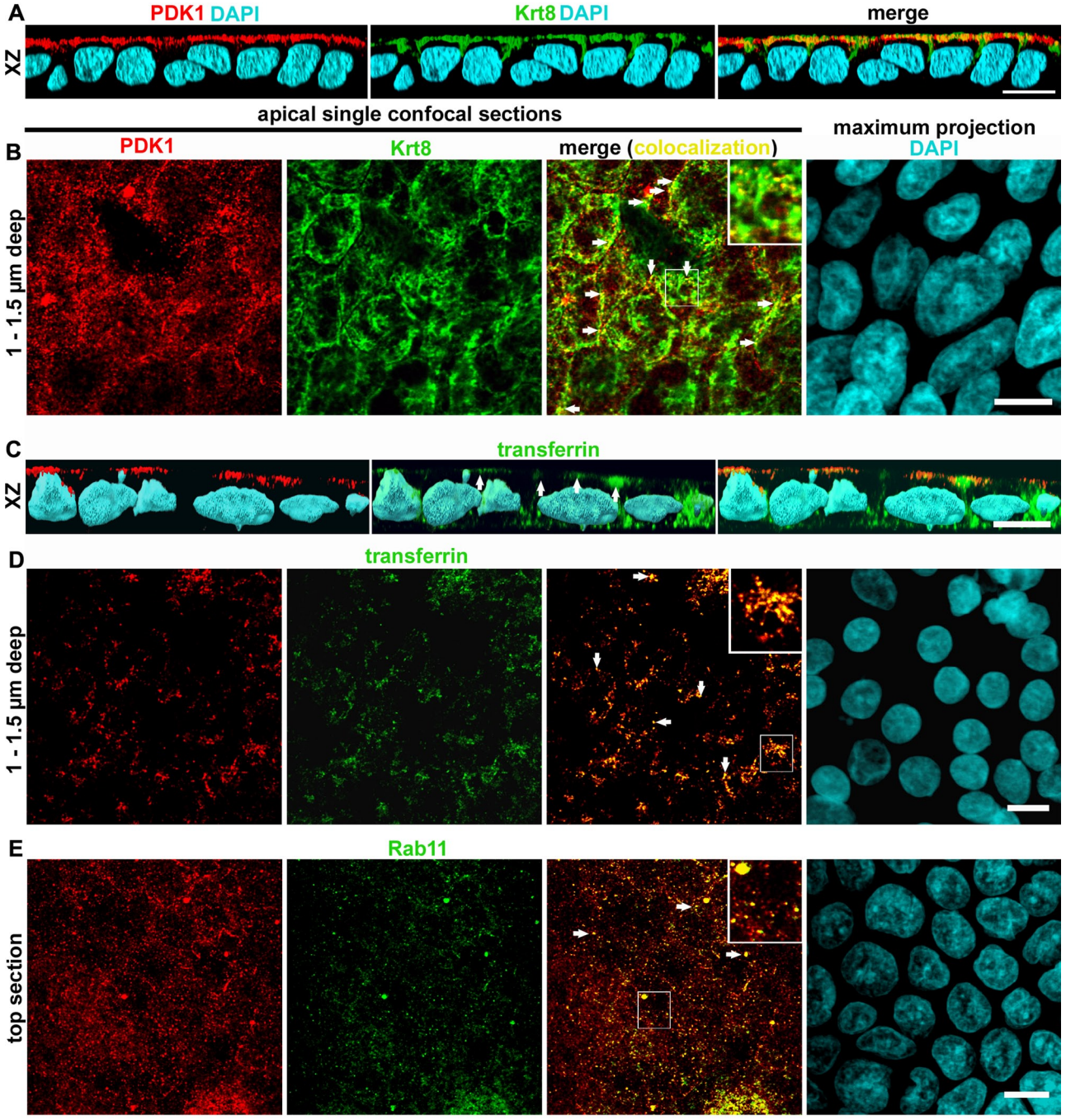

FIGURE 3: PDK1 distributes to an apical vesicular compartment that partially overlaps with endosomes. Confluent differentiated Caco-2 cells grown on filters were analyzed by immunofluorescence against PDK1 (red channel) and other probes under confocal microscopy. (A, C) The *xz* three-dimensional reconstructions of the confocal stacks. (B, D) The *xy* single apical (supranuclear) confocal sections approximately 1–1.5 µm below the plasma membrane (*z* resolution, 0.6 µm). (E) Top section of the stack, showing images that include but are not restricted to the apical plasma membrane. Colocalizations were performed with other proteins in the green channel as follows: (A, B) keratin 8 (Krt8) and (C, D) FITC-transferrin by incubating the cells with the probe from the apical side overnight. (E) Rab11 (ARE marker). In the merged panels, colocalization images appear in yellow. Examples of colocalization are indicated by arrows and enlarged in the inserts. Because the nuclei were located below the sections in all cases, total maximum projection of the 4′,6-diamidino-2-phenylindole (DAPI) signal is shown for each field. Bars, 10 µm; for inserts, 4.3 µm.

The intermediate filament scaffold contains all the components necessary for aPKC refolding rescue except PDK1

On the basis that the IF fraction (P) lacks PDK1 (Figure 2A; Mashukova *et al.*, 2009), we asked whether supplementing this highly insoluble P fraction with recombinant PDK1 would suffice to rephosphorylate IF-bound aPKC. It was demonstrated that P* alone cannot rephosphorylate the attached aPKC (Mashukova *et al.*, 2009). However, in the presence of purified PDK1 the rephosphorylation reaction proceeded normally (Figure 2E, P*

arrowhead). On the other hand, all the known components of the refolding/rephosphorylation machinery are also present in S1, including Hsp70/Hsc70 and soluble aPKC (Mashukova *et al.*, 2009). Furthermore, it is clear from the coimmunoprecipitation results in Figure 1, F and G, that PDK1 and PKCι are already interacting in S1. Thus we supplemented S1 with recombinant PDK1 to the same concentration used in the experiments in Figure 2, C and E. In this case, rephosphorylation of aPKC failed (Figure 3E, S1*, arrowhead), indicating that the filamentous keratin scaffold is essential for the refolding/rephosphorylation machinery to be processive. These results were quantified as a ratio of the pT555 signal to the total PKCι signal (Figure 2F). Supplementing S1* with recombinant PDK1 also served as an important control to show that the rephosphorylation achieved in the in vitro assays shown earlier (Figure 2C and D) is not due to an excessively high, nonphysiological concentration of recombinant PDK1. More important, these experiments allowed us to reach two conclusions: first, that dephosphorylated aPKC bound to IFs at the beginning of the experiment is rescued/processed if PDK1 is added, and second, that the machinery tightly bound to IFs, for example, Hsp70 (Liao *et al.*, 1995; van den Ijssel *et al.*, 1999; Mashukova *et al.*, 2009) and Hsp40 (Izawa *et al.*, 2000), is sufficient to sustain aPKC refolding in a such way that it can be rephosphorylated by PDK1 outside the IFs.

PDK1 is localized to a subapical endosomal compartment and the apical plasma membrane in intestinal epithelial cells

Having confirmed that PDK1 is the kinase involved in maintaining steady-state levels of aPKC in Caco-2 cells, we turned our attention to its subcellular localization. Because IFs are close to but not in direct contact with the plasma membrane, we had two alternative possibilities: either soluble cytosolic or vesicle-associated PDK1 could be in contact with IFs sufficiently close for molecular interactions. The first possibility is functionally viable, since it was shown that PDK1 can phosphorylate the activation domain of some PKC isoforms in a PIP3-independent manner (Sonnenburg *et al.*, 2001), that is, without the need of membrane association. To determine the subcellular localization, we conducted confocal immunofluorescence on filter-grown, differentiated Caco-2 cells. To our surprise, we found that PDK1 localized to the apical pole of the cells in the same region of the terminal web IFs (Figure 3A). Using single confocal *xy*-sections, which have better resolution than the *xz*-sections, we found that PDK1 appeared in puncta, present exclusively in the apicalmost optical sections that comprise the apical surface and the apical region of the cytoplasm (Figure 3, B, D, and E). The distribution of the puncta varied with the depth of the sections, being more homogeneous in the top confocal section, which includes the apical membrane (Figure 3E), and more sparse in the next one to two sections (up to ~1.5 µm below the apical membrane; Figure 3, B and D). Furthermore, PDK1-positive puncta were not observed in confocal sections including the nucleus. We first verified that these vesicle-like PDK1 puncta were indeed in close contact with keratin IFs. In the deepest confocal sections (1–1.5 µm below the surface) in which the PDK1 puncta appear, we found that 42 ± 7% (n = 43 cells) of the puncta colocalized in all or part of their perimeter with keratin filaments (Figure 3B, arrows and insert), indicating that the distance between PDK1 signal and IFs is within the limit of resolution of the confocal microscope.

Then we wanted to identify this novel PDK1 compartment. Our first hypothesis was that PDK1 may be localizing to endosomal membranes. We incubated Caco-2 cells with fluorescent transferrin (Tfn) from the apical side for 2 h. In *xz*-sections, PDK1 signal colocalized with Tfn but only in the apicalmost region of the Tfn compartments (Figure 3C, arrows). Indeed, >50% of the PDK1 puncta found ~1 µm below the apical surface colocalized with transferrin in *xy*-sections (Figure 3D), indicating that a substantial fraction of them correspond to endosomes. No colocalization was observed in deeper sections that included the basolateral Tfn signal. However, because a proportion of the puncta were still not identified, we tested Rab11, a marker of the apical recycling endosome (ARE), which excludes Tfn (Fölsch *et al.*, 2009). Nearly all Rab11-positive puncta were found within the top confocal section that comprises the apical membrane itself. Approximately 80% of the Rab11-positive puncta were also PDK1 positive (e.g., Figure 3E, yellow, arrows and insert). However, only a fraction of the PDK1-positive puncta colocalized with Rab11.

It must be noted that at the conditions in which these confocal images were acquired, the resolution of the instrument in the *z*-axis is approximately 0.5 µm. Therefore it was conceivable that some of the PDK1 puncta in the apicalmost confocal sections may be microvilli at the surface. To test this possibility and verify the immunofluorescence results at much higher resolution, we conducted similar experiments by labeling PDK1 with immunogold for transmission electron microscopy (TEM). The background signal was homogeneously distributed throughout the cytoplasm and the nucleus (Figure 4A), indicating that the antibodies had full accessibility to the entire volume of the cells. The PDK1-specific signal was much higher and heavily concentrated in the apical region of the cells (Figure 4B). When visualized at higher magnification, gold particles showed a striking association with vesicles (Figure 4C) and the apical membrane (Figure 4, B and C, arrows). A morphometric analysis showed 36-fold more PDK1 in the apical membrane than in the lateral membrane (Table 1), confirming that some of the puncta observed by confocal microscopy must correspond to microvilli viewed from above the cell. In fact, the signal associated with the lateral membrane was indistinguishable from the antibody control (nonimmune immunoglobulin G [IgG]). Both basal and nuclear signals were also identical to control levels (Table 1). Finally, 62% of the apical PDK1 signal was associated with vesicles, as opposed to 13% in the antibody control ($p < 0.05$; Table 1). Furthermore, subtracting the vesicle-associated background or the cytosolic background from vesicle-associated and cytosolic PDK1 raw signal, respectively, we

	PDK1	IgG control
Apical membrane (gold particles/µm)	1.1 ± 0.5	0.07 ± 0.1
Lateral membrane (gold particles/µm)	0.03 ± 0.05	0.1 ± 0.09
Supranuclear cytoplasm (gold particles/µm^2)	6.1 ± 2.5	1.5 ± 1.2
Vesicle associated (%)	62 ± 8	13 ± 19
Infranuclear cytoplasm (gold particles/µm^2)	1.0 ± 0.1	1.7 ± 1.6
Nucleus (gold particles/µm^2)	1.7 ± 0.7	1.6 ± 0.6

Membrane association criterion was any gold particle observed in direct contact with a membrane cross section.

TABLE 1: Morphometric analysis of PDK1 distribution in TEM images.

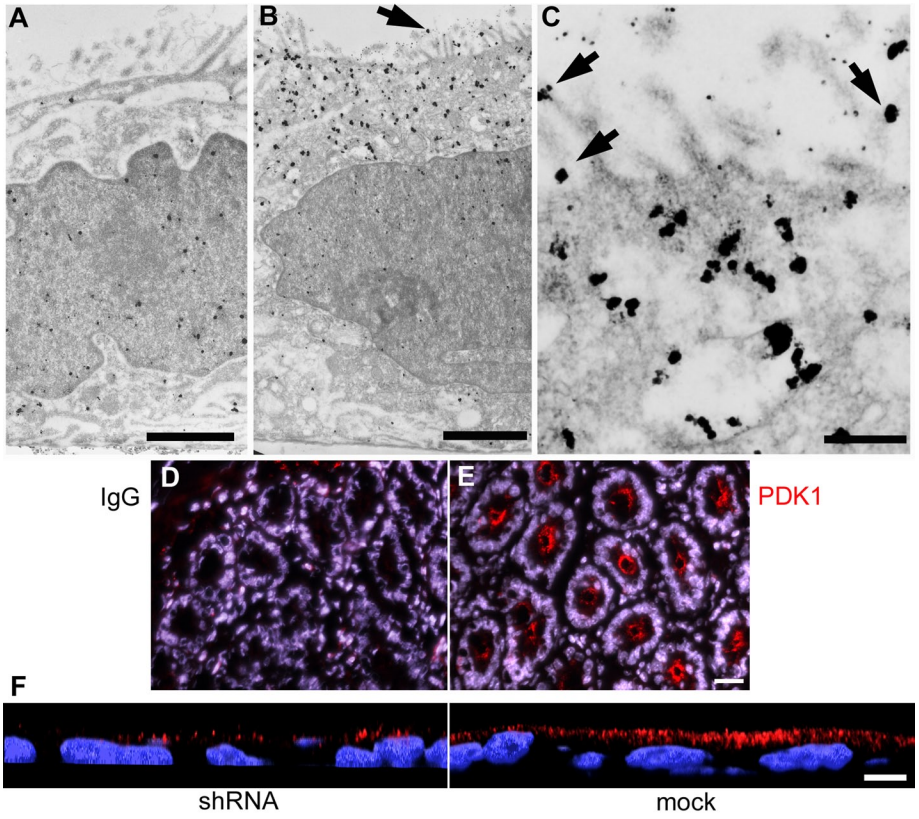

FIGURE 4: PDK1 distributes to a subapical vesicular compartment and the apical plasma membrane in Caco-2 cells and in intestinal crypts. Cultures were processed for immunogold with (A) nonimmune IgG or (B, C) anti-PDK1 antibody, silver enhanced, and viewed under a TEM. Arrows point at apical membrane-associated gold particles. (D, E) Frozen sections of mouse duodenum were processed with (D) nonimmune IgG, or (E) anti-PDK1 antibody (red channel) for immunofluorescence and counterstained with DAPI (blue channel). (F) Confocal *xz*-sections of lentiviral PDK1-knockdown Caco-2 cells (shRNA) or mock-transduced cells processed with the same anti-PDK1 antibody (red channel). Bars, A, 1.4 μm; B, 1.9 μm; C, 0.4 μm; D and E, 20 μm; F, 10 μm.

concluded that 87% of the specific PDK1 signal must be associated to either apical vesicles or the apical membrane. This result confirms the high degree of overall PDK1 membrane compartmentalization observed by confocal microscopy. Taken together, these data show that PDK1 is associated with the apical plasma membrane and apical endosomes, including ARE. Moreover, PDK1 seems to distribute to more than one vesicular compartment, as it also colocalizes with apical vesicles carrying Tfn.

A similar distribution of PDK1 was found in the crypts in frozen sections of mouse duodenum (Figure 4E). On the contrary, the subapical PDK1 compartment was barely visible in the intestinal villi (unpublished data). Because the crypts contain the stem cells and are known to be the proliferative cell population of the intestinal epithelium, this result suggests that the apical arrangement of PDK1 may be associated with proliferative yet polarized epithelial cell populations. Although we performed negative controls with nonimmune IgG for all immunolocalization experiments, we wanted to further control this novel distribution of PDK1 independently. To that end, we processed PDK1-knockdown and mock-transduced Caco-2 cells for immunofluorescence with the same antibodies and procedures. As expected from the effects shown by immunoblot (Figure 1D), the number of PDK1 puncta was greatly reduced in knockdown cells, but their subcellular distribution did not change (Figure 4F).

PDK1 comigrates with endosomal compartments in sucrose gradients

To independently characterize the apical PDK1 membrane compartment, we conducted cell fractionation and separation of endosomal compartments in sucrose gradients by a method developed for polarized epithelial cells in culture (Fialka *et al.*, 1997). This method yielded the Rab11 (ARE) compartment in the top fractions (Figure 5A, control). On the other hand, Tfn endocytosed overnight (basolateral endosomes and CRE) was found in the bottom fractions (Figure 5A, control fractions 5–10). Parallel monolayers were treated with dynasore, a small-molecule inhibitor of dynamin that blocks clathrin-mediated endocytosis (Macia *et al.*, 2006). In these cells, there was no Tfn signal, indicating that indeed the marker was in endosomes and not associated to the plasma membrane (Figure 5A, dynasore).

All detectable PDK1 signal migrated into the gradient in the control cells and was excluded from the top (T) fraction (Figure 5A). Furthermore, PDK1 signal comigrated with Rab11—a marker of ARE—confirming that at least a fraction of the apical vesicles decorated with PDK1 (Figure 3E) corresponds to ARE (Figure 5A, fractions 1–4). A small proportion of the PDK1 signal extended beyond the Rab11 compartment and comigrated with the top Tfn-containing fractions 5–8, confirming the confocal findings in Figure 3, C and D. The bulk of the Tfn-containing compartment (fractions 8–10), however, did not comigrate with PDK1. Of interest, in dynasore-treated cells, a substantial amount of PDK1 did appear in the top fraction of the gradient, suggesting that it is either cytosolic or associated with a very light membrane compartment. It is worth noting that the postnuclear supernatants were normalized by protein content, so that the intensity of the signals cannot be compared for total cell content of these proteins.

Because we noted changes in the distribution of Rab11 itself in the gradients after dynasore treatment, we conducted confocal immunofluorescence experiments. The Rab11 signal was still apical after dynasore treatment but more diffuse than in the control cells, indicating that the dynasore treatment affected the ARE, at least at a structural level (Figure 5B).

The integrity of the PDK1 apical vesicular compartment and its signaling activity is dynamin dependent

Because clathrin-dependent endocytosis and budding from the *trans*-Golgi network are important for membrane traffic into the apical endosomal compartment (Weisz and Rodriguez-Boulan, 2009), we hypothesized that dynasore may functionally disrupt the apical PDK1 compartment. As a matter of fact, dynasore has been found to disrupt apical membrane endosomal recycling in polarized epithelial cells (Cholon *et al.*, 2010). The same overnight treatment in dynasore shown in Figure 5, A and B, resulted in a steep decrease in pT555 and pAkt signals. Total Akt was not affected, whereas PKCι was significantly but modestly decreased (Figure 5, C and D). Of interest,

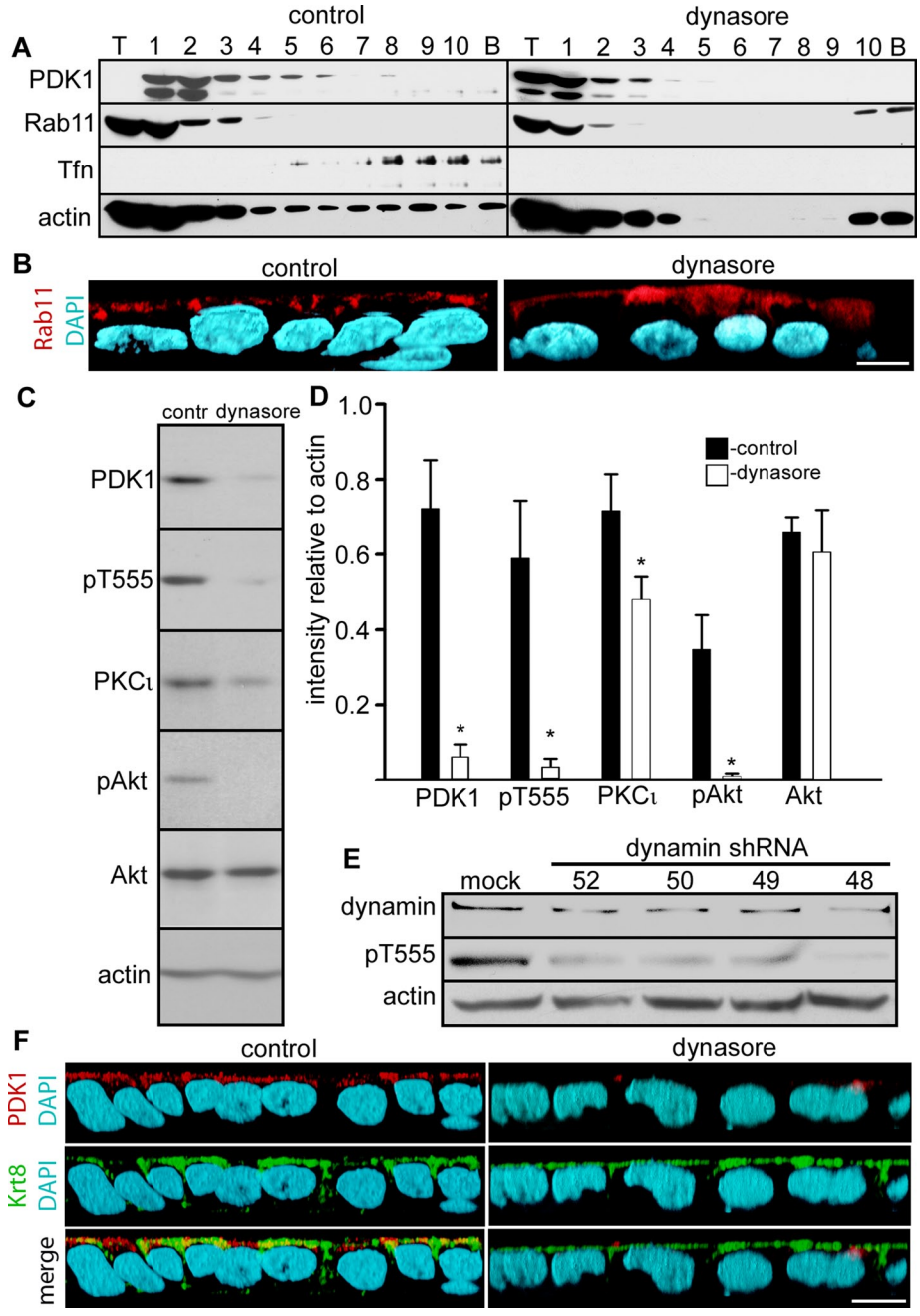

FIGURE 5: PDK1 comigrates with Rab11 and Tfn in sucrose gradients, and its activity is inhibited by dynasore and dynamin 2 knockdown. (A) The postnuclear supernatants of differentiated Caco-2 cells incubated overnight in Tfn from the apical side and treated with 80 μM dynamin inhibitory peptide dynasore or vehicle only (control) were spun on 10–40% continuous sucrose gradients at 100,000 × *g* for 20 h. The gradients were fractionated into one sample of the volume seeded on top (T), 10 identical samples of the gradient (1–10), and a wash of the bottom of the tube (pellet, P). The same blots were sequentially reprobed for PDK1, Rab11, Tfn, and actin. (B) The *xz* reconstructions of confocal stacks of Caco-2 cells grown on filters and treated or not with dynasore were analyzed by immunofluorescence with anti-Rab11 (red channel). (C) Confluent differentiated Caco-2 cells were treated with dynasore or with vehicle DMSO only (contr) in serum-free medium. SDS extracts were analyzed by immunoblot with the antibodies indicated on the left. (D) Quantification of the result shown in C. The bars represent the means ± SD of the ratio of densitometric values of the bands relative to actin bands in the same lane from three independent experiments. For all measurements, nonsaturated images were used (Student's *t* test significance, *p < 0.005 as compared with the corresponding control). (E) Caco-2 cells were transduced with lentiviral particles with no insert (mock) or four different inserts expressing different shRNAs directed against dynamin 2 (52, 50, 49, 48). SDS extracts were analyzed for immunoblot for dynamin 2, pT555 aPKC, and actin. (F) The *xz* three-dimensional reconstruction of a confocal stack. Caco-2 cells grown on filters and treated or not with dynasore were analyzed by immunofluorescence with anti-PDK1 (red channel) and anti–keratin 8 antibodies (Krt8, green channel). Bars, 10 μm.

total PDK1 itself was significantly decreased (Figure 5, C and D). These results contrast with Krt8 down-regulation, which results in a profound decrease in total PKCι with no changes in PDK1 (Mashukova *et al.*, 2009). To verify the specificity of these pharmacological effects, we partially knocked down dynamin 2, the major isoform in epithelia (Chua *et al.*, 2009). Four different shRNAs resulted in knockdowns ranging from 48 to 62%. In all cases, there was a steep reduction in pT555 signal (Figure 5E). The decrease in PKCι total protein was modest (unpublished data), as with dynasore treatment (Figure 5D). Moreover, as expected from the immunoblot analysis, the apical PDK1 compartment was greatly reduced in Caco-2 monolayers incubated in dynasore (Figure 5F). In addition, because the IFs are important in maintaining the steady-state levels of aPKC, we wanted to verify that the dynasore treatment was not affecting the IF cytoskeleton. The IFs remained unchanged and well polarized in cells treated with dynasore (Figure 5F). These results independently confirm the importance of apical endosomes and membrane traffic to sustain PDK1 signaling activity and activation of at least two important targets, aPKC and Akt.

DISCUSSION

The results support two major conclusions: first, that PDK1 is necessary and sufficient to aid the IF-based rescue of PKCι, and second, that PDK1 is exquisitely localized to apical vesicles and apical plasma membrane in intestinal epithelial cells. This is surprising because PDK1 is deemed to be both cytosolic and membrane associated (Pearce *et al.*, 2010). It is also counterintuitive because the main regulator of PDK1 responsible for recruiting PDK1 to the membrane, PIP3, is concentrated in the basolateral domain in polarized epithelial cells (Gassama-Diagne *et al.*, 2006), so that some degree of basolateral localization was expected. Confocal microscopy, immunogold TEM, and sucrose gradient separation of the postnuclear supernatant independently confirmed that only a minimal amount of PDK1 is cytosolic in these cells. Colocalization of PDK1 with apically delivered Tfn and Rab11 suggests a broad localization in endosomes.

Tfn localizes mostly to basolateral endosomes (Fölsch *et al.*, 2009). However, the apicalmost vesicles of this compartment, where PDK1 was found, may correspond to CRE. We have not formally tested all the possible apical vesicular compartments, but the results indicate that PDK1 is not restricted to the ARE. The signaling role of endosomes has been reported in hepatocytes, where EGF receptors (EGFRs) in endosomes signal via PI3K. Of importance, inhibition of endocytosis abrogates that signaling (Luo *et al.*, 2011). The presence of PI3K was demonstrated in clathrin-coated vesicles in nonpolarized cells (Borner *et al.*, 2006). We have not determined whether EGFR is present in the PDK1-positive apical puncta, but it has been known for a long time that EGFR is mostly basolateral in Caco-2 cells and EGF exerts its action only from the basolateral side (Bishop and Wen, 1994). Thus the results suggest that compartmentalization of signaling elements to endosomal vesicles may be a common phenomenon, yet with tissue-specific characteristics.

The mechanism for the apical compartmentalization could involve the weak binding of the PDK1 C-terminal PH domain to phosphatidylinositol (4,5)-bisphosphate (PIP2; Pearce *et al.*, 2010), which is present in apical membranes (Martin-Belmonte *et al.*, 2007), but this still cannot explain its basolateral exclusion. Furthermore, work in other epithelia in vivo suggests that PIP2 may be equally distributed in the apical and basolateral membranes (Ozato-Sakurai *et al.*, 2011). Therefore the PDK1 localization to the apical plasma membrane remains unexplained. Binding of the PH domain to PIP3 is the major force for PDK1 membrane recruitment. PIP3 is present in recycling endosomes (Fields *et al.*, 2010), but its localization specifically to the ARE has not been reported. Of importance, the mechanism that localizes PDK1 is dependent on membrane traffic. Alternatively, it is possible that a more indirect effect of the traffic stoppage resulting from dynasore treatment or dynamin knockdown alters the PDK1 synthesis/degradation balance. It is worth noting that partial PDK1 deficiency impairs specifically apical membrane transport mechanisms in enterocytes (Sandu *et al.*, 2006). Moreover, the presence of Akt2 and PI3K in brush border membranes and early endosomes of intestinal epithelial cells has been reported (Li *et al.*, 2004), thus raising the possibility that apical polarization of the PI3K pathway may be tissue specific and different from the localization in Madin-Darby canine kidney (MDCK) cells.

The dense apical IF network and the abundant apical vesicles localized at the same level are consistent with the model of aPKC refolded by IF-associated Hsp70 (Mashukova *et al.*, 2009) being immediately phosphorylated by PDK1 in adjacent endosomes. This interpretation is also consistent with the results of in vitro rescue of aPKC that failed to show any PDK1 associated to the IFs (Figure 2A) and showed aPKC rephosphorylation totally abrogated by immunodepletion of PDK1 from the Triton X-100–soluble fraction (Figure 2, C and D). At the same time, the fact that soluble recombinant PDK1 was sufficient to enable aPKC rephosphorylation in the IF (pellet; Figure 2, E and F) fraction confirmed that it is the only component missing from the IFs to complete the rescue cycle. Because the rephosphorylated aPKC can only be provided by the IF pellet in the experiments shown in Figure 2E, these results also suggest that the pool of dephosphorylated aPKC bound to IFs (Mashukova *et al.*, 2009) can be rescued and rephosphorylated, and it is not just a "sink" of inactive PKC. In the cell, therefore, PDK1 would be provided by endosomes in the vicinity of IFs, such as those shown in Figure 3B. Functional interactions between endosomes and IFs have been described (Styers *et al.*, 2005; Planko *et al.*, 2007). Conversely, because all the known components of the rescue mechanism (aPKC, Hsp70, PDK1, and ATP) are also present in the soluble (S1) fraction, it remains unsolved what is unique to the IF fraction that enables the reaction to proceed. The identification of PDK1 as the kinase that completes the rescue reaction will facilitate future structural research on how the arrangement of the IF scaffold is necessary for this mechanism. Finally, it is unlikely that our previous results on the role of keratin IFs in aPKC stability are due to effects on PDK1, because Krt8 knockdown did not affect the expression of PDK1, although it substantially decreased the levels of PKCι and Akt. The differences, therefore, suggest that Krt8 knockdown abrogates the chaperoning step, possibly diverting the dephosphorylated kinase molecules to the ubiquitinylation/degradation pathway as shown by proteasome inhibitors (Mashukova *et al.*, 2009). PDK1 inhibition or knockdown analyzed here, on the other hand, is not expected to affect the refolding step but the ensuing rephosphorylation.

Traditionally, membrane traffic has been considered a mechanism to deliver membrane proteins to their specific domains. Our results demonstrate that an acute interruption of the dynamin-dependent traffic also leads to profound changes in PDK1 signaling, as well as in aPKC and pAkt signaling. This opens the possibility that functional consequences of disrupted membrane traffic may arise not only from mislocalized or mistargeted membrane components. Changes in traffic may also cause previously unsuspected fundamental changes in essential signaling pathways. The identification of the traffic-dependent mechanisms responsible for the recruitment and function of PDK1 is well beyond the scope of this work. We can only speculate that dynamin-dependent traffic may be responsible for changes in subcellular localization of PIP3 or perhaps another mechanism for PDK1 recruitment to the membrane. We also speculate that failure of these mechanisms upon interruption of membrane traffic results in a displacement of PDK1 to a different compartment, perhaps as a soluble cytosolic protein, as suggested by the shift to the top fraction of the gradients (Figure 5A), and consequent destabilization. In summary, we found an unsuspected functional connection between membrane traffic, apical endosomal compartments, and aPKC signaling that may also be important for other key pathways such as Akt.

MATERIALS AND METHODS

Antibodies

The antibodies used in this work were as follows: PKCι (BD Biosciences, Franklin Lakes, NJ); pT555 aPKC (Abcam, Cambridge, MA); rabbit anti-PDK1 (Bethyl Laboratories, Montgomery, TX), mouse anti-PDK1 (ECM Biosciences, Versailles, KY); α-tubulin (Sigma-Aldrich, St. Louis, MO); mouse anti-actin (C4; MP Biomedicals, Solon, OH); rabbit polyclonal against active and pro-caspase-3 (Abcam); anti–pan-cytokeratin (Sigma-Aldrich); anti-Krt8 TROMA I (Developmental Studies Hybridoma Bank, University of Iowa, Iowa City, IA); anti-Rab11 (Abcam; Cell Signaling Technology, Beverly, MA); anti-pAkt (Thr-308) and anti-Akt (Cell Signaling Technology); anti-transferrin (Abcam); and anti–dynamin II (BD Biosciences). Secondary fluorescent antibodies were affinity purified and with minimal cross-reactivity for other species (Jackson ImmunoResearch Laboratories, West Grove, PA). Immunogold (Nanogold) antibodies for TEM were obtained from Nanoprobes (Yaphank, NY). Peroxidase-coupled antibodies for chemiluminescence were from KPL (Gaithersburg, MD).

Chemicals and reagents

Chemicals and reagents were used at the concentrations indicated as follows. PDK1 inhibitor, 0.5 μM (BX 912; Axon Medchem, Groningen, Netherlands); EGF (R&D Systems, Minneapolis, MN); dynamin GTPase inhibitor dynasore, 80 μM overnight (Sigma-Aldrich); mTOR inhibitor, 100 nM rapamycin (Sigma-Aldrich); protein synthesis inhibitor, 10 μg/ml cycloheximide (Calbiochem, La Jolla, CA); 150 μM

aPKC substrate peptide (12-536; Upstate, Millipore, Billerica, MA); 0.1 µg/ml recombinant active PDK1 (Abcam; histidine tagged, expressed in Sf9 cells, 123 nmol/min/mg specific biological activity measured by the manufacturer); 5 µg/ml fluorescein isothiocyanate (FITC)–transferrin (Invitrogen, Carlsbad, CA); unlabeled transferrin used for sucrose gradient experiment was from Bio-Rad (Hercules, CA); and 5 µM FITC-phalloidin (Invitrogen). Protease inhibitor cocktail (P-8340; Sigma-Aldrich) and phosphatase inhibitor cocktails (524624 and 52625; Calbiochem) were used according to manufacturer's specifications. The inhibitory PDK1-tide peptide (iPDK1-tide) was myristoylated in the N-terminal end: Myr-KAFCGTPEYLAPEVRREPRILSEEEQEMFRDFDYIADWC. It was obtained from LifeTein (South Plainfield, NJ) and always used at 50 µM. PDK1 activity and the effects of this peptide were measured using the PDK1 Assay/Inhibitor Screening Kit (CycLex, MBL, Woburn, MA) according to manufacturer's protocol. The myristoylated aPKC pseudosubstrate peptide was purchased from Enzo Life Sciences (Plymouth, PA).

Cell culture, immunoblot, immunofluorescence, confocal microscopy, and image analysis

These were all performed as described (Mashukova *et al.*, 2009). Caco-2 human colon carcinoma cells were originally obtained from American Type Culture Collection (Manassas, VA) and cultured from passages 1–25 after the original batch. For immunofluorescence, the cells were fixed in 3% formaldehyde (freshly prepared from paraformaldehyde) and permeabilized in 0.4% Triton X-100, except for Rab11 immunofluorescence. In that case, the fixation was performed in 3% formaldehyde and 0.1% glutaraldehyde, and the cells were permeabilized in 0.4% saponin, continuously maintained in all antibody incubations and washes, instead of Triton X-100.

Immuno–electron microscopy

Immuno–electron microscopy with Nanogold was performed following the protocols suggested by the manufacturer. Briefly, the cells were fixed and permeabilized as described for Rab11 fluorescence. After standard incubations with antibodies, the cells were briefly postfixed in 2% glutaraldehyde, silver enhanced for 2 min, briefly counterstained with 1% OsO_4, and embedded in epoxy resin.

Cell extracts and immunoprecipitation

Nonionic detergent extractions were similar for immunoprecipitation and cell fractionation, followed by in vitro reconstitution. The only difference was that, in the first case, two cocktails of phosphatase inhibitors were used in addition to the cocktail of protease inhibitors. The phosphatase inhibitors were omitted when the cells were extracted for in vitro rephosphorylation assays. In both cases, the cells were extracted in phosphate-buffered saline supplemented with 1% Triton X-100 and 2 mM EDTA and protease inhibitors. For immunoprecipitation, the Triton X-100 extracts were incubated with either rabbit polyclonal anti-PDK1 antibody or with nonimmune IgG. The extracts were then precipitated with protein A beads (Santa Cruz Biotechnology, Santa Cruz, CA) preblocked with 1% bovine serum albumin.

Cell fractionation for cytoskeletal fractions

This was performed as described (Mashukova *et al.*, 2009), a minimal variation of a well-established method to purify intermediate filament keratins (Steinert *et al.*, 1982). Briefly, at 10 d after seeding, Caco-2 cell monolayers were washed in phosphate-buffered saline (PBS) and then extracted in PBS containing 1% Triton X-100 and 2 mM EDTA supplemented with cocktails of protease inhibitors (Calbiochem) at room temperature. After 15 s (three 5-s intervals) of sonication the cell extract was spun for 10 min at 16,000 × *g*. The supernatant was named S1. The pellet was resuspended in 1.5 M KCl in water, sonicated for 15 s (three intervals), incubated for 10 min on ice, and spun for 10 min at 16,000 × *g*. The resulting supernatant was referred to as the S2 fraction, and the pellet was referred to as the P fraction. Triton extraction was performed at room temperature. As a consequence, lipid raft components are present in S1 and S2 and absent from the P fraction (Mashukova *et al.*, 2009).

Subcellular fractionation and separation of endosomes in continuous sucrose gradients

This was performed as described (Fialka *et al.*, 1997; Pasquali *et al.*, 1997) with minimal variations. Only 10 fractions were taken, plus the top of the gradient (supernatant) and the pellet, which was obtained by scraping the bottom of the tube in 1 ml of H_2O. Total ultracentrifugation time was 15 h. Each fraction was trichloroacetic acid precipitated and resuspended in SDS sample buffer for further SDS–PAGE and immunoblot analysis.

Lentiviral infection

PDK1 shRNA lentiviral particles were obtained from Sigma-Aldrich (clone number TRCN0000001476). Dynamin 2 shRNA lentiviral particles were also from Sigma-Aldrich (clones TRCN000006648, 6649, 6650, and 6652). Caco-2 cells were typically infected at 2 d after seeding and selected in 5 µg/ml puromycin for 10 d. Parallel cultures were infected with lentiviral particles carrying no insert (mock infected) and selected in the same way. Knockdown and mock-infected cells were kept in selection medium and used for experiments within the first two passages after infection.

ACKNOWLEDGMENTS

We thank Yolanda Figueroa-Menendez for excellent technical assistance and Margaret Bates for TEM assistance. We also thank Thomas K. Harris and Robert Warren for critically reading the manuscript. TROMA I antibody, developed by P. Brulet and R. Kemler, was obtained from the Developmental Studies Hybridoma Bank. This work was supported by National Institutes of Health Award R01-DK087359 and by a Crohn and Colitis Foundation of America Fellowship to F.A.W.

REFERENCES

Balendran A, Hare GR, Kieloch A, Williams MR, Alessi DR (2000). Further evidence that 3-phosphoinositide-dependent protein kinase-1 (PDK1) is required for the stability and phosphorylation of protein kinase C (PKC) isoforms. FEBS Lett 484, 217–223.

Bayascas JR (2008). Dissecting the role of the 3-phosphoinositide-dependent protein kinase-1 (PDK1) signalling pathways. Cell Cycle 7, 2978–2982.

Bishop WP, Wen JT (1994). Regulation of Caco-2 cell proliferation by basolateral membrane epidermal growth factor receptors. Am J Physiol 267, 5 Pt 1G892–G900.

Borner GH, Harbour M, Hester S, Lilley KS, Robinson MS (2006). Comparative proteomics of clathrin-coated vesicles. J Cell Biol 175, 571–578.

Cameron AJ, Escribano C, Saurin AT, Kostelecky B, Parker PJ (2009). PKC maturation is promoted by nucleotide pocket occupation independently of intrinsic kinase activity. Nat Struct Mol Biol 16, 624–630.

Cholon DM, O'Neal WK, Randell SH, Riordan JR, Gentzsch M (2010). Modulation of endocytic trafficking and apical stability of CFTR in primary human airway epithelial cultures. Am J Physiol Lung Cell Mol Physiol 298, L304–L314.

Chua J, Rikhy R, Lippincott-Schwartz J (2009). Dynamin 2 orchestrates the global actomyosin cytoskeleton for epithelial maintenance and apical constriction. Proc Natl Acad Sci USA 106, 20770–20775.

Fialka I, Pasquali C, Lottspeich F, Ahorn H, Huber LA (1997). Subcellular fractionation of polarized epithelial cells and identification of organelle-specific proteins by two-dimensional gel electrophoresis. Electrophoresis 18, 2582–2590.
Fields AP, Regala RP (2007). Protein kinase C iota: human oncogene, prognostic marker and therapeutic target. Pharmacol Res 55, 487–497.
Fields IC, King SM, Shteyn E, Kang RS, Fölsch H (2010). Phosphatidylinositol 3,4,5-trisphosphate localization in recycling endosomes is necessary for AP-1B–dependent sorting in polarized epithelial cells. Mol Biol Cell 21, 95–105.
Fölsch H, Mattila PE, Weisz OA (2009). Taking the scenic route: biosynthetic traffic to the plasma membrane in polarized epithelial cells. Traffic 10, 972–981.
Gassama-Diagne A, Yu W, ter Beest M, Martin-Belmonte F, Kierbel A, Engel J, Mostov K (2006). Phosphatidylinositol-3,4,5-trisphosphate regulates the formation of the basolateral plasma membrane in epithelial cells. Nat Cell Biol 8, 963–970.
Gao T, Newton AC (2006). Invariant Leu preceding turn motif phosphorylation site controls the interaction of protein kinase C with Hsp70. J Biol Chem 281, 32461–32468.
Gao X, Harris TK (2006). Steady-state kinetic mechanism of PDK1. J Biol Chem 281, 21670–21681.
Gould CM, Newton AC (2008). The life and death of protein kinase. *C*. Curr Drug Targets 9, 614–625.
Ikenoue T, Inoki K, Yang Q, Zhou X, Gua K-L (2008). Essential function of TORC2 in PKC and Akt turn motif phosphorylation, maturation and signalling. EMBO J 27, 1919–1931.
Izawa I, Nishizawa M, Ohtakara K, Ohtsuka K, Inada H, Inagaki M (2000). Identification of Mrj, a DnaJ/Hsp40 family protein, as a keratin 8/18 filament regulatory protein. J Biol Chem 275, 34521–34527.
Le Good JA, Brindley DN (2004). Molecular mechanisms regulating protein kinase Cζ turnover and cellular transformation. Biochem J 378, 83–92.
Leontieva OV, Black JD (2004). Identification of two distinct pathways of protein kinase Cα down-regulation in intestinal epithelial Cells. J Biol Chem 279, 5788–5801.
Li X, Leu S, Cheong A, Zhang H, Baibakov B, Shih C, Birnbaum MJ, Donowitz M (2004). Akt2, phosphatidylinositol 3-kinase, and PTEN are in lipid rafts of intestinal cells: role in absorption and differentiation. Gastroenterol 126, 122–135.
Liao J, Lowthert LA, Ghori N, Omary MB (1995). The 70-kDa heat shock proteins associate with glandular intermediate filaments in an ATP-dependent manner. J Biol Chem 270, 915–922.
Luo Y, Cheng Z, Dixon CJ, Hall JF, Taylor E, Boarder MR (2011). Endosomal signalling of epidermal growth factor receptors contributes to EGF-stimulated cell cycle progression in primary hepatocytes. Eur. J Pharm 654, 173–180.
Macia E, Ehrlich M, Massol R, Boucrot E, Brunner C, Kirchhausen T (2006). Dynasore, a cell-permeable inhibitor of dynamin. Dev Cell 10, 839–850.
Martin-Belmonte F, Gassama A, Datta A, Yu W, Rescher U, Gerke V, Mostov K (2007)). PTEN-mediated apical segregation of phosphoinositides controls epithelial morphogenesis through Cdc42. Cell 128, 383–397.
Mashukova A, Oriolo AS, Wald FA, Casanova ML, Kröger C, Magin TM, Omary MB, Salas PJ (2009). Rescue of atypical protein kinase C in epithelia by the cytoskeleton and Hsp70 family chaperones. J Cell Sci 122, 2491–2503.
Mashukova A, Wald FA, Salas PJ (2011). TNF-α and inflammation disrupt the polarity complex in intestinal epithelial cells by a post-translational mechanism. Mol Cell Biol 31, 756–765.
Newton AC (2010). Protein kinase C: poised to signal. Am J Physiol Endocrinol Metab 298, E395–402.
Ozato-Sakurai N, Fujita A, Fujimoto T (2011). The distribution of phosphatidylinositol 4,5-bisphosphate in acinar cells of rat pancreas revealed with the freeze-fracture replica labeling method. PLOS One 6, e23567.
Pasquali C, Fialka I, Huber LA (1997). Preparative two-dimensional gel electrophoresis of membrane proteins. Electrophoresis 18, 2573–2581.
Pearce LR, Komander D, Alessi DR (2010). The nuts and bolts of AGC protein kinases. Nat Rev Mol Cell Biol 11, 9–22.
Peifer C, Alessi DR (2008). Small-molecule inhibitors of PDK1. ChemMedChem 3, 1810–1838.
Planko L, Böhse K, Höhfeld J, Betz RC, Hanneken S, Eigelshoven S, Kruse R, Nöthen MM, Magin TM (2007). Identification of a keratin-associated protein with a putative role in vesicle transport. Eur J Cell Biol 86, 827–839.
Sandu C, Artunc F, Palmada M, Rexhepaj R, Grahammer F, Hussain A, Yun C, Alessi DR, Lang F (2006). Impaired intestinal NHE3 activity in the PDK1 hypomorphic mouse. Am J Physiol Gastrointest Liver Physiol 291, G868–G876.
Smith L, Wang Z, Smith JB (2003). Caspase processing activates atypical protein kinase C ζ by relieving autoinhibition and destabilizes the protein. Biochem J 375, 663–671.
Sonnenburg ED, Gao T, Newton AC (2001). The phosphoinositide-dependent kinase, PDK1, phosphorylates conventional protein kinase C isozymes by a mechanism that is independent of phosphoinositide 3-kinase. J Biol Chem 276, 45289–45297.
Steinert P, Zackroff R, Aynardi-Whitman M, Goldman RD (1982). Isolation and characterization of intermediate filaments. Methods Cell Biol 24, 399–419.
Styers ML, Kowalczyk AP, Faundez V (2005). Intermediate filaments and vesicular membrane traffic: the odd couple's first dance? Traffic 6, 359–365.
Suzuki A, Ishiyama C, Hashiba K, Shimizu M, Ebnet K, Ohno S (2002). aPKC kinase activity is required for the asymmetric differentiation of the premature junctional complex during epithelial cell polarization. J Cell Sci 115, 3565–3573.
Suzuki A, Ohno S (2006). The PAR-aPKC system: lessons in polarity. J Cell Sci 119, 979–987.
Tanentzapf G, Tepass U (2002). Interactions between the crumbs, lethal giant larvae and bazooka pathways in epithelial polarization. Nat Cell Biol 5, 46–52.
van den Ijssel P, Norman DG, Quinlan RA (1999). Molecular chaperones: small heat shock proteins in the limelight. Curr Biol 9, 3R103–R105.
Wald FA, Oriolo AS, Mashukova A, Fregien NL, Langshaw AH, Salas PJ (2008). Atypical protein kinase C (iota) activates ezrin in the apical domain of intestinal epithelial cells. J Cell Sci 121, 644–654.
Wald FA, Forteza R, Didwadkar-Watkins R, Mashukova A, Duncan R, Abreu MT, Salas PJ (2011). Aberrant expression of the polarity complex atypical PKC and non-muscle myosin IIA in active and inactive inflammatory bowel disease. Virchows Arch 459, 331–338.
Wang Q, Margolis B (2007). Apical junctional complexes and cell polarity. Kidney Int 72, 1448–1458.
Weisz OA, Rodriguez-Boulan E (2009). Apical trafficking in epithelial cells: signals, clusters and motors. J Cell Sci 122, 4253–4266.
Zhang L *et al.* (2006). Integrative genomic analysis of protein kinase C (PKC) family identifies PKCiota as a biomarker and potential oncogene in ovarian carcinoma. Cancer Res 66, 4627–4635.